

A Thesis Report on
**Modelling and Experimental Study for the Design and Development of
the Heat Receiver Tube for Solar Concentrator**

Submitted in partial fulfilment of requirement for the award of degree of

**MASTER OF ENGINEERING
IN
CAD/CAM ENGINEERING**

Submitted by

RUPINDER SINGH

Roll No. 801481019

Under the Guidance of

Dr. V.P Agrawal

Visiting Professor,

Mechanical Engineering Department,

Thapar University, Patiala

Mr. Sandeep Kumar

Visiting Professor,

Mechanical Engineering Department,

Thapar University, Patiala



DEPARTMENT OF MECHANICAL ENGINEERING

Thapar University, Patiala

June, 2016

DECLARATION

I hereby declare that work done in the thesis entitled, “Modelling and Experimental Study for the Design and Development of the Heat Receiver Tube for Solar Concentrator” is an authentic record of work carried out by me under the supervision of Dr. V.P. Agrawal and Mr. Sandeep Kumar.

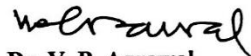
Date: 08/07/2015



RUPINDER SINGH

Roll No. 801481019

This is to certify that above declaration made by the student concerned is correct to the best of our knowledge and belief.



Dr. V. P. Agrawal

Visiting Professor

Mechanical Engineering Department

Thapar University, Patiala



Mr. Sandeep Kumar

Visiting Assistant Professor

Mechanical Engineering Department

Thapar University, Patiala

Countersigned by:



Dr. S.K. Mohapatra

Senior Professor and Head

Mechanical Engineering Department,

Thapar University, Patiala



Dr. S.S. Bhatia

Dean of Academic Affairs,

Thapar University, Patiala

ACKNOWLEDGMENT

I am going to take the privilege of thanking all those people who have helped me to put all the ideas and work, well above the level of simplicity and into something concrete.

First of all, I would like to express my sincere thanks to **Dr. V. P .Agrawal** for his guidance and advice during my thesis work. As my supervisor, he has constantly encouraged me to remain focused on achieving my goal.

I thank whole heartedly, **Mr. Sandeep Kumar** for constantly motivating me for doing better and showing complete confidence in my work. As my Co-supervisor, he has extended appropriate help at every point which has proved very relevant in understanding the problem area and working on the solution. In addition to his guidance; his constant encouragement, observations and comments have helped me to follow the right direction in the research and to move forward with an investigation in depth. He has helped me greatly and been a source of knowledge. Also in the process, I learnt a lot on other technical and non-technical things from him.

I wish to thanks **Dr. Madhup Kumar Mittal** and **Mr. Gurbinder Singh** for giving their valuable suggestions and help me in the experimental work, whenever I approached them.

I must acknowledge all the help in form of academic or non-academic resources that I have got from my institute **Thapar University, Patiala**. I would like to thank all the administrative and technical staff members of the Department who has been kind enough to advise and assist in their respective roles.

At last, but not the least, I would like to thanks my all family members for supporting me in my all works, wherever I needed. Specially, I wish to thanks my friend **Bikramjeet Makkar, Gurminder Panesar, Paramdeep Dhillon, Ramneet Brar, Baltej Rupal, Karan Saini, Harman Sekhon, Jashan Sharma** for motivating me to done this work and making my two year in college grateful.

Rupinder Singh

Rupinder Singh

ABSTRACT

Solar energy is the most abundant form of renewable energy. Solar energy has been used in different form from the ages. The variation in the solar incident radiation *w.r.t.* day time, location and season has attracted the researchers towards harnessing the solar energy in most optimum way. Harnessing energy in the form of heat has been of prime importance. Apart from flat plate collectors, solar concentrator technology (Linear Fresnel collector, parabolic dish collector, parabolic trough collector, heliostat field collector) are used to concentrate the solar radiation energy in order to enhance the heat transfer and system efficiency.

Various types of a heat absorbing fluid (with higher thermal conductivity and specific heat) are used in a concentrator like Nano-fluid, water, Ethylene Glycol, Therminol VP-1 etc. Enhancing the heat transfer capacity has been prime research area in order to achieve higher efficiency and performance at reduced cost.

Present work is focused on the design and development of a receiver tube that can be used for PTC. Thermal properties like thermal conductivity, specific heat capacity, and density and flow properties like mass flow rate, flow turbulence has been studied and evaluated for the optimum heat transfer for the variety of fluids. CFD modelling of a fluid flow and heat transfer using ANSYS FLUENT software has been performed. Solar radiation for input heat and K- ϵ model for the turbulence has been invoked in the present modeling work for simulating the various real time situations. There is a lack of sufficient and authentic data in the literature to validate the model. Thus, for the validation of the model, own setup of PTC is used to perform experiments with different fluid (Water, Ethylene Glycol, and Therminol VP-1) by varying the flow rate and by creating the turbulence in the fluid flow in pipe. Experimental result data and fluid properties are used for simulation and validation of the CFD model.

The present work intends to develop a universal model that can be used to identify dimensions, suitable working fluid and flow properties to achieve optimum solar heat collection at a given geographical location.

Contents

DECLARATION.....	ii
ACKNOWLEDGMENT.....	ii
ABSTRACT.....	iv
Contents	v
List of Figures.....	vii
List of Tables	viii
Nomenclature	ix
1 Introduction.....	1
1.1 Introduction	1
1.2 Solar Energy	1
1.3 Solar Collectors	2
1.4 Parabolic Trough Collector	3
1.5 Different Heat Transfer Fluids	4
1.6 CFD Modeling.....	5
1.6.1 Surface to Surface Radiation model [12].....	6
1.6.2 Assumptions of Surface to surface model [12].....	6
1.6.3 Limitation of Surface to Surface model [12]	6
1.7 Scope of the Thesis	6
1.8 Organization of the thesis.....	7
2 Literature Survey	9
2.1 Introduction	9
2.2 Review related to CFD Modelling	9
2.3 Review related to Experimentation	12
3 Experimental Setup	16
3.1 Introduction	16
3.2 Parabolic Trough Collector	16
3.3 Components of Parabolic Trough Collector	17
3.2.1 Reflector.....	17
3.2.2 Tracking System	18
3.2.3 Absorber Tube	18
3.4 Specifications of the Experimental Setup	19
3.5 Heat Transfer Fluid	20
3.6 Summary	21

4 CFD Methodology	22
4.1 Introduction	22
4.2 Philosophy of Computational Fluid Dynamics	22
4.3 Governing Equations	23
4.4 Methodology of CFD	24
4.5 Geometric Modelling	24
4.6 Meshing	25
4.7 Steps to solve the problem using FLUENT module in ANSYS	26
4.6.1 Read the Mesh File and check grid quality	27
4.6.2 Model Defining	27
4.6.3 Selection of the Material	27
4.6.4 Boundary Conditions	28
4.6.5 Solution Initialization and Run calculation	28
5 Results and Discussion.....	29
5.1 CFD Modeling Results	29
5.1.1 Case 1: Water with flow velocity of 0.066 m/s	29
5.1.2 Case 2: Water with flow velocity of 0.11 m/s	30
5.1.3 Case 3: Ethylene Glycol with flow velocity of 0.066m/s	31
5.1.4 Case 4: Ethylene Glycol with flow velocity of 0.11m/s	32
5.1.5 Case 5: Therminol VP-1 with flow velocity of 0.066 m/s	33
5.1.6 Case 6: Therminol VP-1 with flow velocity of 0.11 m/s	33
5.1.7 Case 7: Mythol Therm 500 with flow velocity of 0.066 m/s	34
5.1.8 Case 8: Mythol Therm 500 with flow velocity of 0.11 m/s	35
5.2 Experiment Procedure	36
5.3 Experiment Results	36
5.3.1 Variation of Output Temperature with Time	36
5.3.2 Variation of Efficiency with Time	38
5.4 Validation with CFD Modelling Results	41
5.5 Summary	43
6 Conclusions.....	44
6.1 Conclusion.....	44
6.2 Future Scope.....	45
References.....	47
Appendix A.....	51
Appendix B.....	53

List of Figures

Figure 1.1 Schematic of a Parabolic trough collector [3].	4
Figure 1.2 Temperature range of different HTF's. [10].	5
Figure 3.1 Parabolic Trough Collector	17
Figure 3.2 Stepper Motor	18
Figure 3.3 Heat Absorbing Element	19
Figure 4.1 Three Dimensions of Fluid Dynamics	22
Figure 4.2 Geometric model of HAE	25
Figure 4.3 Meshed geometry of Heat absorbing element	25
Figure 4.4 Front view of meshed geometry	26
Figure 5.1 Temperature Contour when the water flow rate 0.066 m/s	29
Figure 5.2 Temperature Contour when the water flow rate 0.11 m/s	30
Figure 5.3 Temperature contour when EG flows at 0.066 m/s	31
Figure 5.4 Temperature contour when EG flows at 0.11 m/s	32
Figure 5.5 Temperature contour when Therminol VP-1 flows at 0.066 m/s	33
Figure 5.6 Temperature contour when Therminol VP-1 flows at 0.11 m/s	33
Figure 5.7 Temperature contour when Mythol Therm 500 flows at 0.066 m/s	34
Figure 5.8 Temperature contour when Mythol Therm 500 flows at 0.11 m/s	35
Figure 5.9 Output Temperature of different fluid at velocity 0.066 m/s	37
Figure 5.10 Output Temperature of different fluid at velocity 0.11 m/s	38
Figure 5.11 Efficiency variation with varying Solar Radiation at day time with velocity 0.066 m/s	39
Figure 5.12 Efficiency variation with varying Solar Radiation at day time with velocity 0.11 m/s	40
Figure 5.13 Comparison between CFD model and Experimental Energy gain	42

List of Tables

Table 1.1 Solar energy collectors [2].	3
Table 3.1 Specification of experimental setup	19
Table 3.2 Thermo-Physical properties of Fluids	21
Table 4.1 Meshing Details	26
Table 4.2 Volume and Area Statistics	27
Table 4.3 Thermo-physical properties of various material used in CFD simulation	28
Table 5.1 Modelling results of water with different flow rates	30
Table 5.2 Modelling result with different flow rate of Ethylene Glycol	32
Table 5.3 Modelling result of Therminol VP-1 with different flow rates	34
Table 5.4 Modelling result with different flow rates of Mythol Therm 500 oil	35
Table 5.5 Average efficiency of PTC during Morning, Noon and Full Time	40
Table 5.6 Comparison of CFD Model and Experimental Results	42
Table A.1 Water with flow rate 0.066 m/s	51
Table A.2 Ethylene Glycol with flow rate 0.066 m/s	51
Table A.3 Therminol VP-1 with flow rate 0.066 m/s	52
Table A.4 Mythol Therm 500 with flow rate 0.066 m/s	52
Table B.1 Water with flow rate 0.11 m/s	53
Table B.2 Ethylene Glycol with flow rate 0.11 m/s	53
Table B.3 Therminol VP-1 with flow rate 0.11 m/s	54
Table B.4 Mythol Therm 500 with flow rate 0.11 m/s	54

Nomenclature

List of Abbreviation

CFD	: Computational Fluid Dynamics
CSP	: Concentrated Solar Power
HTF	: Heat Transfer Fluid
PTC	: Parabolic Trough Collector
TES	: Thermal Energy Storage
Re	: Reynolds Number
W1	: Water with flow velocity 0.066 m/s
EG1	: Ethylene Glycol with flow velocity 0.066 m/s
MT1	: Mythol Therm 500 with flow velocity 0.066 m/s
TH1	: Therminol VP-1 with flow velocity 0.066 m/s
W2	: Water with flow velocity 0.11 m/s
EG2	: Ethylene Glycol with flow velocity 0.11 m/s
MT2	: Mythol Therm 500 with flow velocity 0.11 m/s
TH2	: Therminol VP-1 with flow velocity 0.11 m/s

List of Symbol

ρ	: Density
u	: Velocity in x-direction
δ_{ij}	: Intermolecular Distance
T	: Temperature
g_i	: Gravitational Acceleration
λ, C_p	: Constant
S_T	: Momentum Source

Chapter 1

Introduction

1.1 Introduction

Energy is one of the most important driver force of the development of a nation. On the other hand, environmental problem increases dramatically in order to fulfill the energy demand. Main cause of this is increasing population, energy consumption and industrial activities. Use of fossil fuel as a source of energy pollutes the environment day by day. As per review, 76 million barrels of oil is consumed across the worldwide daily [1]. By using these non-renewable energy sources of energy we are compromising with the life of our new generation. On the other hand renewable energy is collected from the natural resources like wind, sun, and hydro and is abundantly available. Use of renewable energy is environment friendly. Sun has the store of a large amount of a clean energy available on earth. This clean energy reaches the earth in the form of radiation. These radiation energy stored or collected in the form of heat energy. Though the solar energy is being used from primitive time but it has generated special interest today due to rise in pollution or environmental problem, and most of the countries are committed for research in this area to develop the sustainable source of energy.

1.2 Solar Energy

The Sun is the major source not only for direct solar energy, but is also indirectly responsible for wind, tidal, bioenergy etc. The Sun is the largest member of a solar system which is approximately 99% mass of a solar system. It is spherical in shape with 1.39×10^9 m radius filled with the hot gas and plasma matter. Nuclear fusion reaction in which helium atom converts into hydrogen, is the source of all the continuous solar energy released. Sun is an effective black body with the surface temperature of 5762 K [1]. Temperature at the center of a sun is very high as

compared to the surface temperature which is at approx. 8×10^6 to 40×10^6 K. The Sun emits its energy in the form of radiation in direction outward which is equal to the 63 MW/m^2 of the sun surface. Only the small fraction of this energy, approx. 1.7×10^{14} kW, strikes the earth surface [1]. It is estimated that the annual demand for energy of world is equal to the 30 min of radiation strikes on the surface of earth [1].

Energy emitted by the sun can be calculated by using the Stephen Boltzmann law of radiation.

$$E = \epsilon \sigma T^4 \quad (1)$$

Where

ϵ = Surface Emissivity

σ = Stephen Boltzmann Constant, $5.67 \times 10^{-8} \text{ W/m}^2\text{k}^4$

1.3 Solar Collectors

Harnessing solar energy efficiently is one of the prime areas of research. The major component of any solar system is a solar collector or concentrator. Solar collectors, an important component of any solar devices, absorb/focus the radiation incoming from the sun and transfer the heat to a transporting material like oil, water and air as internal energy. The absorber can take a variety of configurations. It can be cylindrical or flat.

Basically solar collectors are of two types

- Non- concentrating or Stationary
- Concentrating

Comprehensive list of these collectors are shown in table 1.1.

Table 1.1 Solar energy collectors [2].

Type	Motion	Collector	Absorber type
Non-Concentrating	Stationary	Flat plate collector	Flat
		Evacuated tube collector	Flat
		Compound parabolic	Tubular
Concentrating	Single-axis tracking	Linear Fresnel reflector	Tubular
		Parabolic trough collector	Tubular
		Cylindrical trough collector	Tubular
	Double-axis tracking	Parabolic dish reflector	Point
		Heliostat field collector	Point

In the present work, we are mainly focus on the Parabolic trough collector because of it has a good efficiency as compare to the other concentrating collector and requires only single axis tracking. Most of the researchers are working on this technology commercially. Most important factors for the efficiency of the solar device is design of the solar collector and absorber tube, concentration ratio of a reflecting surface and thermo-physical properties of heat transfer fluid. From the literature, it is evident that efforts are on different designs are being developed for the absorber tube and developing new heat transfer fluid.

1.4 Parabolic Trough Collector

The parabolic trough collector is made up of a reflecting sheet such as a glass sheet or polished metallic sheet bent into a parabolic shape. The absorber tube is placed at the focal line of this parabola and covered with the glass tube to reduce the convective heat loss [3]. Schematic diagram of PTC is shown in Figure. 1.1.

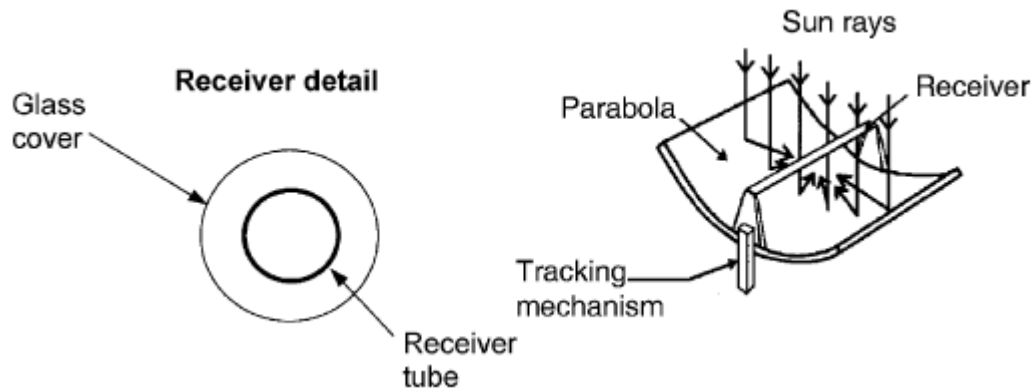


Figure 1.1 Schematic of a Parabolic trough collector [3].

Tracking mechanism of parabolic trough collector can be divided into electronics/electrical and mechanical [3]. From these two categories electronic tracking system is more accurate and reliable. In electronic tracking mechanism, stepper motor is electronically controlled by the micro-controller, which gives the step size to motor relative to the sun speed. In the second case a signal is given to the motor by sensor, which detects the solar flux intensity on the receiver tube [4].

Parabolic trough collector is a good technology to generate the temperature up to 400 °C. Biggest application of system of this type is Southern California power plants, which is known as solar electric generating system. It has the power production capacity of 354 MW. Spain has developed this system only for experimental purpose with the total power producing capacity of 1.2 MW [5, 6].

1.5 Different Heat Transfer Fluids

Heat transfer fluid (HTF) is the major component of a parabolic trough collector which transports the heat energy. Efficiency of the PTC depends on HTF. Many types of a HTF are used in PTC like water, oil, air. Researchers working in this domain are trying to improve the thermal properties of a these fluid. Latest work is on a Nano-fluid. In this, a small Nano particle of metal like Al, Cu, and Ag are added or suspended in to the base fluid like water, ethylene glycol or any thermal oils. It improves the thermal properties like thermal conductivity, viscosity, specific heat capacity etc. But, there is some problems using Nano fluid i.e. agglomeration and

unstable mixing (Particle settle down), increasing pumping power, erosion- corrosion of heat transfer element [7]. Linear relationship is develop between thermal conductivity and volume concentration of Nano particle (Al_2O_3 , commonly used) using water [8]. It has been reported that if the transformer oil is used as base fluid instead of water with Al_2O_3 particle, then the thermal conductivity is doubled [9].

Apart from these heat transfer fluid molten metal and molten salts are also used as a heat transfer fluid. Molten salt has a good heat storage capacity. *Andasol-1* is used as the HTF in a plant situated in Spain, operation by the end of 2008, has commercially proven the molten salt as an effective heat transfer fluid [10, 11]. Molten salt has a high temperature range and it is cheaper relatively to other heat transfer fluid. But, the problem with molten salt as a HTF is corrosion of container and piping alloys. Temperature range of various HTF's are shown in figure 1.2.

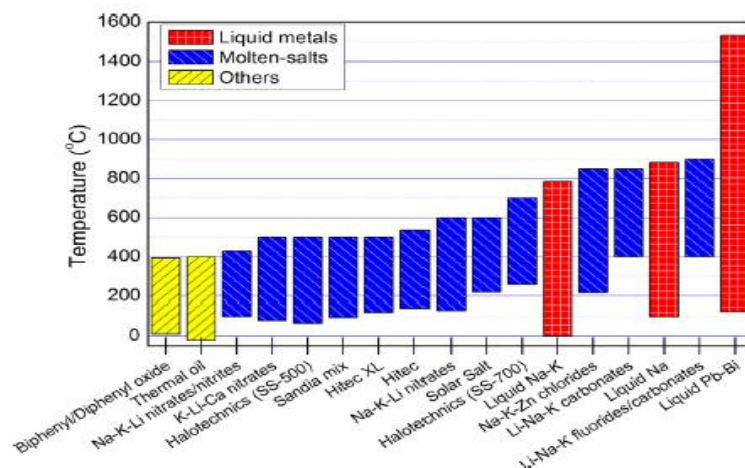


Figure 1.2 Temperature range of different HTF's. [10]

1.6 CFD Modeling

Computational fluid dynamics model of heat absorbing element of PTC is modeled using ANSYS Fluent module. For the radiation different model like P-1 model, DTRM model, Rosseland model, S2S model. But from the literature, for the modeling of a heat absorbing element with solar radiation surface to surface model is used, because it is a more accurate and suitable for this problem.

1.6.1 Surface to Surface Radiation model [12]

The surface to surface radiation model can be used for the radiation exchange between the diffused gray surface clusters. The energy transformation between two surfaces depends upon their size, orientation, separation distance etc. All these parameter are accounted or solved by a geometric function known as a “view factor”.

1.6.2 Assumptions of Surface to surface model [12]

- Surface to surface model assumes the surface to be diffused and gray. The feature of gray surface is that its absorptivity and emissivity are independent of the wavelength.
- Any absorption, scattering of the radiation is ignored and the only surface to surface radiation are consider for the analysis.

1.6.3 Limitation of Surface to Surface model [12]

- It does not support hanging nodes, non-conformal interface.
- It is not used for model participating radiation problem.
- This model cannot be used if the model contains periodic and symmetric boundary conditions.
- Memory requirement in CPU storage increase rapidly if the number of surfaces are increase. This is minimized by using the clustering of the surface faces.

1.7 Scope of the Thesis

World demand rate for the energy is increase day by day because of population burst and the technological advancement. Therefore, it is important to go for a reliable, cost effective and everlasting renewable resource of energy to fulfill the demand of energy. Solar energy resource is one of the most beneficial energy resource as

compare to another resources because it is free and easily available energy resource. To collect the solar energy different types of technologies are developed.

From all these technology concentrating solar power (CSP) technology is most promising and the most of the researcher are working on this technology. Parabolic trough collector is based upon the CSP technology. Researcher has developed different numerical model for study the parameter of a parabolic trough collector. Some researcher performed experiments to check the thermal efficiency of a parabolic trough collector with different the heat transfer fluid. They are using water, air, thermal oil, molten salt etc. Nano particles are suspended in the base fluid like water to enhance the thermal properties of the fluid. In the present work, main focus is done on the CFD model being developed for the design of heat absorbing element (HAE) and to check the performance of the PTC. Experiments have been performed with different heat transfer fluid (HTF) to validate the CFD model.

Application of this model in future will be for developing a heat absorbing element and for collector size or dimension. By simply varying the input parameter like climate condition or solar radiation intensity, power requirement etc. in the model.

1.8 Organization of the thesis

The organization of the thesis given below:

In **Chapter 2**, discusses on the work which are done by the different authors in the field of concentrating solar energy. Different numerical, CFD models are studied and their results are discussed. Experimental work on the parabolic trough collector by using different conditions, materials etc are referred and discussed.

In **Chapter 3**, presents the experiment setup, its components and design specifications etc., which are used in the present work to validate the CFD modeling results from ANSYS.

In **Chapter 4**, methodology of the CFD model formulation is discussed step by step using ANSYS Fluent module. These steps considering the geometric modeling of the HAE, meshing of the geometric model, boundary conditions etc. are explained in details.

In **Chapter 5**, results from the CFD model using ANSYS and the results from experiments are discussed and compared.

In **Chapter 6**, conclusion and future scope of the thesis are pointed.

Chapter 2

Literature Survey

2.1 Introduction

In this chapter, literature review and experimentation of heat absorbing element is discussed. At the outset of the chapter, review related to CFD modeling is elaborated author wise, in which main focus is considered on the surface to surface radiation modeling. The attempt is made to find the limitation in the CFD modeling of heat absorbing element. In the second subsection of this chapter, experimentation problems are discussed, which has been performed by several researchers. Different researchers has used different types of materials for heat absorbing tube, such as copper, stainless steel, brass, etc. along with different type of absorbing fluid materials such as, Nano fluid, thermal oil, molten salt, water, air, etc.[13,14,15,16]. The conclusions from the literature survey are drawn at the end of this chapter.

2.2 Review related to CFD Modelling

Tijani A. S et al [17]. Absorber tube of a parabolic trough collector is modeled in ANSYS with the same geometry of LS-2 parabolic trough collector. In boundary condition for the simplification of model some assumptions are made i.e. solar radiation flux is assumed uniform around the tube. In this, investigate the effect of a varying wind speed, flow rate of a heat transfer fluid on the heat loss by using the surface to surface solar radiation model. From the results it is observe that wind speed and flow rate are not very large effect on the solar radiation, but the convective losses contribute in the large heat loss. For the wind speed of 2 m/s, 36% of a total heat loss contribute by radiation and the 64% by convection heat loss. At flow rate 0.04 kg/s heat loss is rise from 198W/m to 2010 W/m with small amount but at flow rate of 0.8 kg/s the total loss increase by about 4.8%.

H Yurong et al [18]. Single phase and combined discrete and continuous models are performed to study the heat enhancement by using the TiO₂ nanoparticle which are flowing through the uniformly heated tube. In this, investigate the concentration of nanoparticle, Reynolds number and particle size on the convective heat transfer. Validating the numerical results with the experimental result and get the good relation between these two. From the results state that the thermal conductivity is more affected on the heat transfer as compare to the viscosity, lift force, thermophoretic force, Brownian force.

Rios Iribe E Y et al [19]. CFD study has been used for the heat transfer and pressure drop using non Newtonian fluid, which are flow through the circular pipe of a uniform wall temperature. A helical strip with different twist ratios are inserted in the tube for producing the swirl in flow and change the Reynolds number from 0.2-600. Helical strip generate the velocity gradient with tube wall, which consequently affect the heat flow rate. From the results observed that there is a good agreement between the CFD result and theoretical results. Results indicate the by decreasing the twist ratio and increasing the Reynolds number the thermo-physical performance can be increased.

Moraveji M K et al [20]. In this article studied that a nanofluid with nanoparticle of Al₂O₃ (Average size 45 and 150 nm) with the base fluid water used as a heat transfer fluid flowing through the constant heat flux tube using CFD. Effect on heat transfer with concentration 1,2,4,6 % by weight and the Reynolds number ($500 < Re < 2500$) for the different axial location of pipe. By using the results equation for Nusselt number are obtain for predicting the dimensionless number. Predicted results has a very good relationship with the experimental result obtained from the literature. 10% error between the experimental and predicted results.

Mwesigye A et al [21]. Monte Carlo Ray Tracing (MCRT) method is used to calculate the heat flux which is concentrate on the receiver tube. MCRT method is used with computational fluid dynamics tool for evaluate the temperature and thermal performance of parabolic trough collector. In this Cu nanoparticles are used with the base fluid THERMINOL-VP1 oil as heat transfer fluid. Temperature range at inlet of receiver is 350-650 K and the flow rates in the range of 1.22-135 m³/h. From the numerically results observed that thermal performance is increases by increase the

volume fraction of nanoparticle. Thermal efficiency of PTC is increases by 12.5% when the concentration rise from 0 to 6 %. Entropy can be generated above the certain value of a Reynolds number.

Fard M H et al [22]. Comparison of single phase and two phase model using the CFD result and these result compare with the experimental result. A Nano fluid flowing through the uniformly heated tube is modeled by CFD. Single phase and double phase model are used to calculate the heat transfer rate and the effect of some parameter such as nanoparticle size, concentration, peclet number on the heat transfer. It is observed that heat transfer rate increase by increase in the concentration and by peclet number. Results shows that the two phase model give better result as compare to single phase model. Double phase model give the nearer result to the experiment. Error between single phase model and experimental results are 16% and in the case of two phase model this error approximately 8%.

Yaghoubi et al [23]. Experiment is conduct to validate the numerical results for the heat loss of a receiver tube of a parabolic trough collector. In which receiver tube is covered with the glass tube. Gap between the glass tube and receiver tube is filled in one case is vacuum and in second case gap is filled with air. The temperature of glass tube is measured with the help of infrared thermograph. From the results observed that in the case of vacuum convective heat loss is less as compare to in the case of air. Results shows that heat loss in case of air is 40% higher than the case of vacuum by this the efficiency of collector reduce by 3-5 %.

Natarajan et al [24]. The numerical simulation is carried out using ANSYS CFX 12.1 software for the convective heat transfer in receiver tube of a parabolic trough collector by creating the obstruction of different cross section in the path of flow. The material of the absorber tube is copper and the fluid flowing is a water. Meaning of obstruction is to create the turbulence in the flow. SST $k-\omega$ model is used to modelling of turbulence. Heat transfer and pressure drop characteristics are calculated for the fluid flow rate 85Kg/hr and solar irradiance of 850 W/m². Triangular and semi-circle shapes are insert for the study purpose. It is observed that by triangular shape insertion heat transfer rate is uniform as compare to any other shape and thermal fatigue is less in the case of triangle. Pressure drop is high in the case of insertion compared to without insertion

2.3 Review related to Experimentation

Anton J M et al [25]. Use of the gas in the PTC as a heat transfer fluid has a good advantages as compare to the use of oil. A testing setup is built up at platform a solar de Almeria for check the technically feasibility of the new technology. In the case of oil there is limitation of a temperature range but in the case of gas temperature range is very high. Due to this thermal efficiency of system increases. Very high working pressure reduce the pumping power.

Wu Y T et al [26]. An experiment is performed to check the performance and heat loss in parabolic trough collector using molten salt as a heat transfer fluid. By this experiment also calculate the value of convective heat transfer to HTF and total heat transfer coefficient of the water to salt heat exchanger. From the results observed that heat loss in heat absorbing element is more as compare to PTR70 and 5% of the total loss in a tube is at the joints. The value of heat transfer coefficient in water to salt heat exchanger is lies between 600 to 1200 W/m²K. From the results observed that the experimental system shows the good agreement with existing very important correlation presented by the Sieder-Tate equation and the Gnielinski equation. Results for the heat loss from molten salt as a HTF serves as a good reference for the further practically or commercialized application.

Zhang H et al [27]. In this paper, comparison of numerically 1-D and 3-D model results with the experimental setup results exited at the Sandia National Laboratory. From the results observed that difference of the temperature at the output of a receiver tube is 0.65⁰ C in the case of 1-D model. But in the case of 3-D model the difference of temperature is about 2.69⁰ C. So, from the results we can say that the 1-D model gives better results as compare to the 3-D model. Assumption for the 1-D model is, convective heat transfer between the glass and tube annulus, conduction through glass cover, absorber and support brackets; radiation in the annulus and from the glass to the sky. Assumptions in the case of 3-D model is more as compare to the 1-D model. Hence, error is large in the case of 3-D model.

Jiang Y et al [28]. The use of conventional flat plate collector for water heating system in the cold places is less efficient because of low efficiency, large heat loss, tube burst and freeze. To overcome these problem a small sized parabolic trough collector is developed for the water heating at cold places. The experimental setup is

developed under the condition of cold place for observe the characteristics of PTC. Results shows the efficiency of collector is 67% when the solar radiation is less than 310 W/m^2 . Which indicate that the collector collect the radiation efficiently. From the results observed that by increase the Reynolds number thermo-physical properties of HTF can improve and when the temperature of a working fluid is less than 100^0 C then the efficiency of PTC is improved with the rise in temperature of the working fluid.

Behar O et al [29]. Numerically Novel PTC model has develop for the validation of model, the results of the model compare with the experimental test results conduct by the Sandia National Laboratory during the LS-2 test at AZTRAK platform. From these two observe the good agreement between the results. For the case of receiver coated with cermet the results of Novel PTC model is compare with the results of Energy Equation Solver (EES) code developed by National Renewable Energy laboratory (NREL), the comparison between two shows improves thermal efficiency of the collector. It is observed that Novel parabolic trough model gives the better result for thermal efficiency as compare to EES model with the uncertainty of 0.64% compare to EES 1.11%. In this paper survey also related to the design of parabolic trough collector to make it promising technology.

Shafii M. B et al [30]. From the recent investigation studied that a parabolic trough collector used for water desalination system. In this, parabolic trough collector is utilizes with the heat pipe and two evacuated annular glass tube. Results shows that the production rate of a purified water and the efficiency of system is $0.27 \text{ Kg/m}^2\text{h}$ and 22.1% when the aluminum foil is inserted between the gap between the two glass tube and the value of these two when the annular gap is filled with the oil is $0.933 \text{ kg/m}^2\text{h}$ and 65.2%.

Larcher M et al [31]. An experiment is conduct for theinvestigate the optical efficiency on the basis of optical behavior of collector at high and low temperature condition and also the heat loss from the receiver tube when the temperature is high and no radiation. Efficiency is calculate for the operating temperature up to 200^0 C and on measurement to determine the value of incidence angle modifier (IAM).

Alguacil M et al [32]. The use of parabolic trough collector for direct steam generation (DSG) is not a commercialized system till yet. But, to check the

performance of the DSG system a demonstration plant is setup by the Abengoa solar. Temperature range is high to make the steam superheated it's about 500⁰C to 700⁰C. To control the saturated steam large control system is required. To overcome this problem, Albengoa solar built a small scale demonstration plant of 8 MWht. This demonstration plant working at 85 bar and 4500C has been operated and evaluated for one year.

Cheng et al [33]. Large number of experiment is conducted for the comparison, sensitive analysis and design optimization of a parabolic trough collector. Six different parabolic trough collector named as LS-2, LS-3, Sky Trough, Euro Trough, LAT 73, Helio Trough and Ultimate Trough along with four different receiver tube named as LS-2 receiver, LS-3 receiver, Siemens UVAC 2010 receiver and Schott PTR 70 receiver. From the results it was found that UVAC 2010 receiver absorb large amount of a heat energy and the LAT 73 has the best optical efficiency as compare to other collector.

2.4 Conclusion from Literature Review and objective of the thesis

The literature review in present work suggests that a significant amount of experimental work has been performed in the field of solar energy using PTC with variety of heat transfer fluid. The literature related to modeling work is limited towards focus on development of a design specific model.

Present work has identified some research gaps related to modeling towards design of PTC. Present work focuses on the design of absorber tube which functions as heat transfer tube with concentrated solar heat falling on the outer surface and heat being removed through heat transfer fluid (HTF). The design aspect of thermo-physical properties of the HTF, the flow rate and the location of the system installation are majorly focused in the present work. The modeling work need some data to verify the model and author found the lack of all the availability of necessary data in the literature. So, the present thesis also focuses on the experimental work using PTC installed in Energy Lab in Thapar University. The working parameters and the initial

and boundary conditions are derived from the own experiments to validate the CFD model developed.

Chapter 3

Experimental Setup

3.1 Introduction

In this chapter, experimental setup and its specific details are discussed. At the outset of this chapter, parabolic trough collector (PTC) setup is described along with its components. Further, design specifications for the PTC are listed on the basis of reflector dimensions, absorber tube material, control unit, storage unit and temperature sensors. Different types of heat transfer fluids used are discussed.

3.2 Parabolic Trough Collector

A parabolic Trough collector (PTC) is made by bending the sheet of a reflecting material in the parabolic shape. Reflecting material may be a polished mirror, aluminum sheet, etc. In present work, reflecting surface is made by using polished stainless steel material due to its non-corrosive property and high reflectivity 0.84. Radiation from the sun enters or falls on the trough parallel to its plane of symmetry. From the trough surface these radiation are reflected or concentrated to its focal line. A receiver tube is placed along the focal line of parabola. The receiver tube or the absorber tube is covered by the concentric glass cover tube to reduce the convective loss. The heat transfer fluid which is flowing through the absorber tube get heated to a high temperature and rise heat energy by the concentrated radiation of Sun. Sun is track in the east-west direction. Parabolic trough collector test rig is as shown in Figure 3.1.



Figure 3.1 Parabolic Trough Collector

3.3 Components of Parabolic Trough Collector

Three main component of PTC are listed below:

- Reflector
- Tracking System
- Heat Absorber Tube

3.2.1 Reflector

Reflecting surface is the most important component for the working of a parabolic trough collector. So, for the reflection the material which has the high reflectivity are used. In the present work reflector made up with the Stainless steel of reflectivity near to one. Dimension of the reflector given in the Table 3.1.

3.2.2 Tracking System

The collector is oriented in the North-South direction and tracks in the East-West direction by using the micro-controller. Main component of a tracking system is a stepper motor is shown in a Figure 3.2. Stepper motor is used to rotate the reflector for tracking the sun with minimum step size of 0.004° . The advantage of this tracking mechanism is that the small adjustment is required during the start of the day of experiment. Span for track the sun is 40° east to 40° west. Tracker is move accordance with the sun speed i.e. reflector cover 15° in one hour with the speed of sun.



Figure 3.2 Stepper Motor

3.2.3 Absorber Tube

It is also known as the receiver of the PTC. It is placed along the focal line of a parabola. Absorber tube is the most important element of the system. Material of the absorber tube has good thermal properties. It has a good thermal conductivity, in the present case we are using the copper tube with the diameter of 0.031 m . To increase the absorptivity of the copper tube is electroplated with the nickel and chromium. Receiver tube is covered with the glass tube of the outer diameter 0.0504 m to reduce the convective heat loss from the receiver tube.



Figure 3.3 Heat Absorbing Element

3.4 Specifications of the Experimental Setup

Specifications of the component of PTC are listed below in the Table.3.1.

Table 3.2 Specification of experimental setup

S. No.	Components	
1	Parabolic Reflector	Specification
	Length	1.219 m
	Arc Length	1.829 m
	Depth	0.207 m
	Focal Length	0.607 m
	Material	SS with mirror film
	Tracker	Single axis (E-W)
	Reflectivity	0.84
2	Absorber Tube	Specification
	Length	1.219 m
	Diameter	0.031 m
	Absorber Tube material	Copper & SS
	Insulation material	PUF
	Piping Material	GI and copper
3	Storage Unit	Specification
	Storage Tank	2(One with heat exchanger and one without heat exchanger)

	Capacity	28 Liter
	Material	SS
	Insulation of Tank	Glass Wool with Rexene
4	Control Unit	Specification
	Stepper Motor	1 (For Tracking)
	Pump (for water)	
	Power Rating	0.1 HP
	Head	5 m
	Pump (for oil)	
	Power Rating	0.5 HP
	Head	10 m
5	Sensing Element	Specification
	RTD Sensor	To measure temperature
	Flow Meter	To measure fluid flow rate
	Pyranometer	To measure solar radiation intensity
	Anemometer	To measure wind velocity

3.5 Heat Transfer Fluid

It is the fluid flowing through the receiver tube and carries the heat from the receiver tube. In the present work four different fluid are used. Fluid has categorized in the two type

1. Water based
 - Water
 - Ethylene Glycol
2. Oil Based
 - Therminol VP-1
 - Mythol Therm 500

All the fluid has there different physical chemical properties to check the performance of PTC and the effect of heat transfer fluid by changing the flow rate. Thermo-physical properties of fluid are given in the Table.3.2.

Table 3.3 Thermo-Physical properties of Fluids

Fluid Name	Thermal Conductivity(W/m-K)	Sp. Heat(KJ/Kg-K)	Density(Kg/m ³)
Water	0.622	4.18	1000
Ethylene Glycol	0.254	2.43	1110
Therminol VP-1	0.117	2.27	1068
Mythol Therm 500	0.102	2.15	868

3.6 Summary

Parabolic trough collector with the reflecting surface of stainless steel material and the material of heat absorbing tube is copper are used in the experiment. Tracking of the collector with respect to the sun position is done by the stepper motor. Which are controlled by the controller. Four types of the heat transfer fluid (Water, Ethylene glycol, Therminol vp-1, Mythol therm 500) are used for testing.

Chapter 4

CFD Methodology

4.1 Introduction

This chapter represents the work related to modeling of computational fluid dynamics (CFD). The philosophy of CFD is discussed at the outset, which further leads to governing equation and methodology. Different steps followed to develop the CFD model in ANSYS FLUENT such as geometry development, meshing, boundary conditions are well described for developing the CFD technique is presented.

4.2 Philosophy of Computational Fluid Dynamics

Computational Fluid Dynamics (CFD) is a most important tool for solving the fluid flow problem. It constitutes new “third approach” in the development of the whole discipline of the fluid dynamics. In 1960’s the researcher focused on the two approaches i.e. theoretical and experimental. But today CFD approach has equal partnership for solving the fluid dynamics problem with pure theory and experiment approach. Advancement in a fluid dynamics in future is depends upon all three approaches as shown in figure 4.1. CFD helps to analyse and understand the result from experiment and theory, and vice versa.

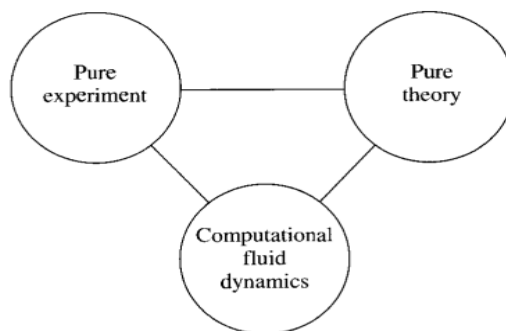


Figure 4.1 Three Dimensions of Computational Fluid Dynamics

CFD has a many application like in Automobile and engine, Industrial Manufacturing, Civil Engineering, Environment Engineering etc.

4.3 Governing Equations

In CFD physical aspects of a fluid flow are governed by three fundamental principal, first principal is mass conserved, second is conservation of momentum and third is energy conservation.

The Governing equation of fluid flow and heat transfer is a mathematical formulation of the laws of conservation of fluid mechanics and these equations referred to as Navier- Stokes equations.

These governing conservations equation can be written as:

Continuity equation:

$$\frac{\partial \rho}{\partial t} + \frac{\partial}{\partial x_i} (\rho u_i) = 0 \quad (1)$$

Momentum equation:

$$\frac{\partial}{\partial t} (\rho u_i) + \frac{\partial}{\partial x_i} (\rho u_i u_j) = \frac{\partial}{\partial x_j} \left[-\rho \delta_{ij} + \mu \left(\frac{\partial u_i}{\partial x_j} + \frac{\partial u_j}{\partial x_i} \right) \right] + \rho g_i \quad (2)$$

Energy equation:

$$\frac{\partial}{\partial t} (\rho c_p T) + \frac{\partial}{\partial x_i} (\rho u_i c_p T) - \frac{\partial}{\partial x_j} \left(\lambda \frac{\partial T}{\partial x_j} \right) = s_T \quad (3)$$

4.4 Methodology of CFD

All CFD code mainly contains three important steps

1. Pre processor

- Definition of the geometry of the region of interest
- Meshing: Sub division of domain into small number of domain.
- Specification of appropriate boundary conditions

2. Solver

- Integration of the governing equation of fluid flow over all the control volume of domain
- Discretization- conversion of the resulting integral equations into system of algebraic equation
- Solution of algebraic equation by iterative method

3. Post processor

- Domain geometry and grid display
- Vector, Contour and other plot to display the results

4.5 Geometric Modeling

Domain of interest in parabolic trough collector is its heat absorbing element. We can analyze it by creating the model of the heat absorbing element. Geometry of the heat absorbing element of a PTC is created using the Geometric modeling module in the ANSYS software. Geometry of HAE is consist of a simple circular pipe of a length 1219 mm and diameter of 31 mm. Glass Tube cover is made up of 50.4 mm & 45.1 mm external and internal diameter. Profile of the geometry is shown in Figure 4.2.

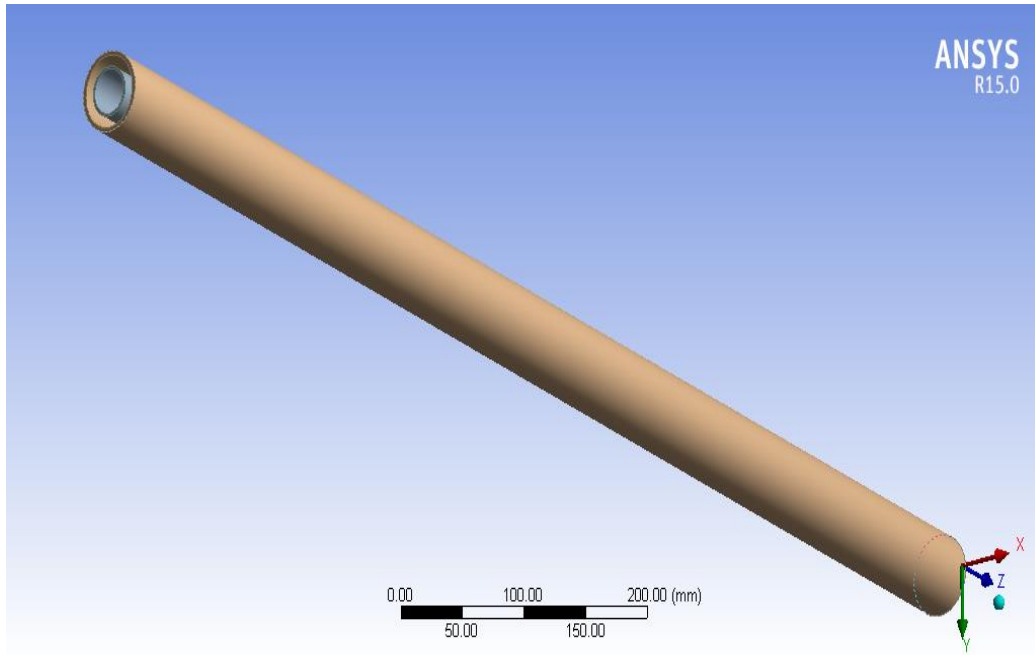


Figure 4.2 Geometric model of HAE

4.6 Meshing

It is the discretized model of the heat absorbing element into a small number of a domain. In the present work mesh is develop using meshing module in the ANSYS software. Automatic method is adopted to create the mesh. Isometric view is shown in Figure 4.3. And the front view is as shown in Figure 4.4.

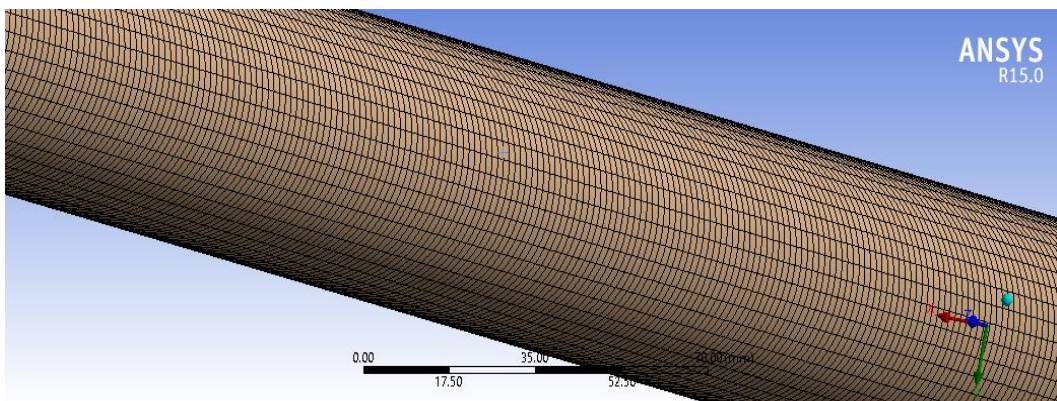


Figure 4.3 Meshed geometry of Heat absorbing element

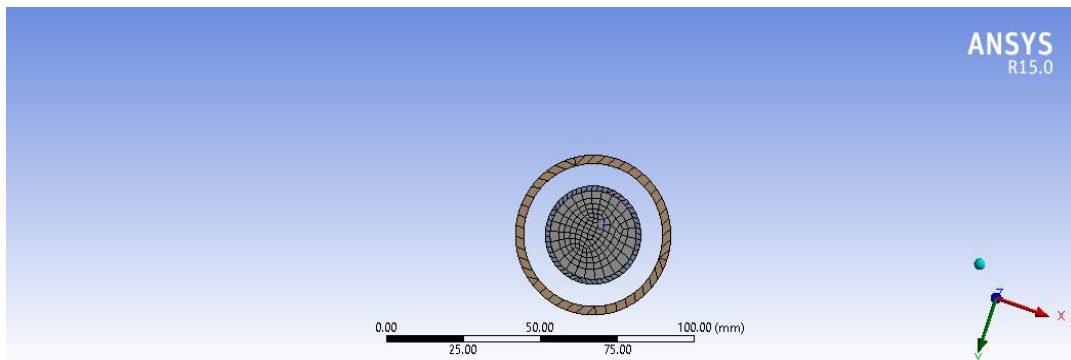


Figure 4.4 Front view of meshed geometry

Table 4.1 Meshing Details

Nodes	746676
Elements	134802
Mesh Metric	Skewness
Minimum	1.029e-02
Maximum	0.614
Average	0.243
Standard Deviation	0.148

4.7 Steps to solve the problem using FLUENT module in ANSYS

Steps to solve the problem in Fluent are written on next pages.

4.6.1 Read the Mesh File and check grid quality

Table 4.2 Volume and Area Statistics

Volume Statistics	
Minimum Volume (m ³)	1.937432e-09
Maximum Volume (m ³)	3.672120e-08
Total Volume (m ³)	1.091073e-03
Area Statistics	
Minimum Face Area (m ²)	1.291621e-06
Maximum Face Area (m ²)	1.233207e-05

4.6.2 Model Defining

In the Present simulation model Energy equation is ON. Laminar flow is consider through the pipe. Surface to surface radiation model is on in which solar load is applied using solar ray tracing method and calculate the view factor. Participating Zone in the view factor calculation is the outer wall of the tube.

4.6.3 Selection of the Material

Following types of material are used in CFD Simulation

- Water
- Ethylene Glycol
- Therminol VP-1 oil
- Mythol Therm-500 oil
- Copper

Table 4.3 Thermo-physical properties of various material used in CFD simulation

Material Name	Thermal Conductivity(W/m-K)	Sp. Heat(KJ/Kg-K)	Density(Kg/m ³)
Water	0.622	4.18	1000
Ethylene Glycol	0.254	2.43	1110
Therminol VP-1	0.117	2.27	1068
Mythol Therm 500	0.102	2.15	868
Copper	387.6	0.381	8978

4.6.4 Boundary Conditions

In the boundary conditions, Inlet and heat flux input values are given. In the present work flow at the inlet is maintained as uniform mass flow by varying the velocity by 0.022 m/s, 0.066 m/s, 0.11 m/s and 0.15 m/s. Pressure at the outlet is specified as zero bar (gauge pressure). No slip condition is used for the wall motion.

For the heating radiation is on by taking the value of internal and external emissivity as constant. Define the shell conduction up to one layer of thickness 1.375 mm.

4.6.5 Solution Initialization and Run calculation

Standard Initialization are taken for the current problem and after the initialization calculation are run for convergence.

Chapter 5

Results and Discussion

In this chapter, CFD modeling using ANSYS Fluent results and the experiment results are given with the different cases of fluids. Procedure follows to perform the experiment are given in this chapter. In the results efficiency of the system and the maximum temperature gain are calculated. For the validation of the CFD model, at the last of this chapter comparison between the CFD and experiment results are given. The Summary is drawn in the end of this chapter.

5.1 CFD Modeling Results

Methodology or steps to solve the CFD problem in ANSYS Fluent are given in the Chapter 4. Simulation is run for the eight different case and the results of them are given next in this chapter.

5.1.1 Case 1: Water with flow velocity of 0.066 m/s

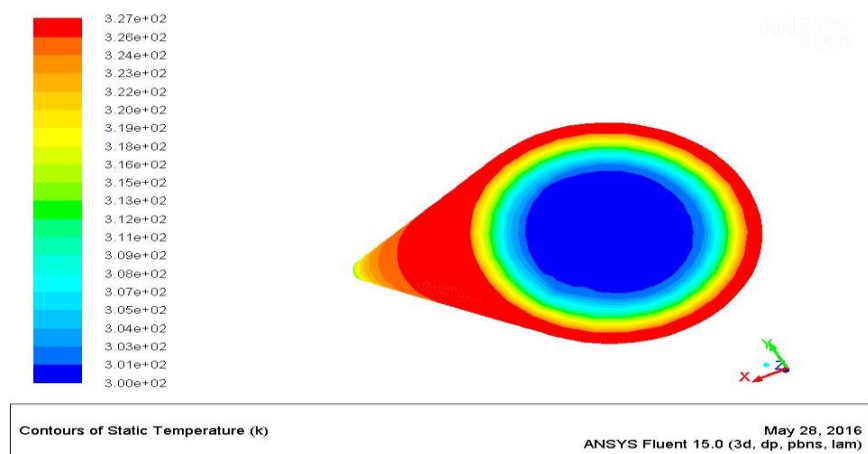


Figure 5.1 Temperature Contour when the water flow rate 0.066 m/s

At the flow rate of 0.066 m/s of water the temperature profile is as shown in the Figure4.5. Maximum temperature of a water is achieved at the outlet of pipe. Flow through the tube is a laminar. The rise in temperature from inlet to outlet in a single pass is equal to 3.4 °C. Contour shows the temperature of the water increase gradually. Surface temperature of the tube is approximately equal to the 48 °C

5.1.2 Case 2: Water with flow velocity of 0.11 m/s

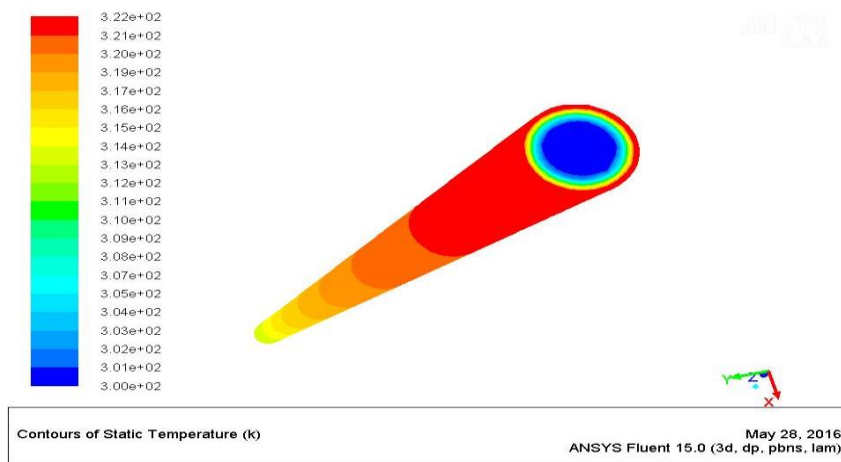


Figure 5.2 Temperature Contour when the water flow rate 0.11 m/s

In this case maximum temperature of the water is at the outlet of a tube and the rise in a temperature is equal to the 1.89°C in a single pass through the tube. From the results observed that as the increase in a flow rate the then the rise in a temperature of a water is decreases.

Table 5.1 Modelling results of water with different flow rates

Flow rate (m/s)	Inlet Temperature	Outlet temperature	Tube Wall Temperature
0.022 (1 LPM)	300 K	306.6 K	319.83 K
0.066 (3 LPM)	300 K	303.4 K	320.7 K
0.11 (5 LPM)	300 K	301.89 K	317.6 K
0.15 (7 LPM)	300 K	301.36 K	316.34 K

5.1.3 Case 3: Ethylene Glycol with flow velocity of 0.066m/s

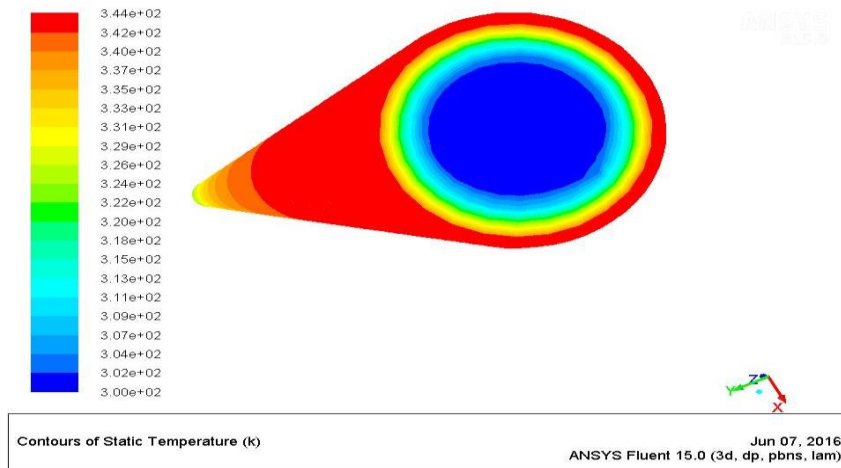


Figure 5.3 Temperature contour when EG flows at 0.066 m/s

At the flow rate of 0.066 m/s of ethylene glycol the contour of temperature is as shown in the Figure 4.7, the figure shows that the temperature of fluid is gradually increase from inlet to outlet as well as radially inward decreased. The temperature rise in the single pass is equal to 4.9°C. Temperature gain in single pass of ethylene glycol through the pipe is more as compare to the water. The surface temperature of the tube wall is approximately equal to the 62°C.

5.1.4 Case 4: Ethylene Glycol with flow velocity of 0.11m/s

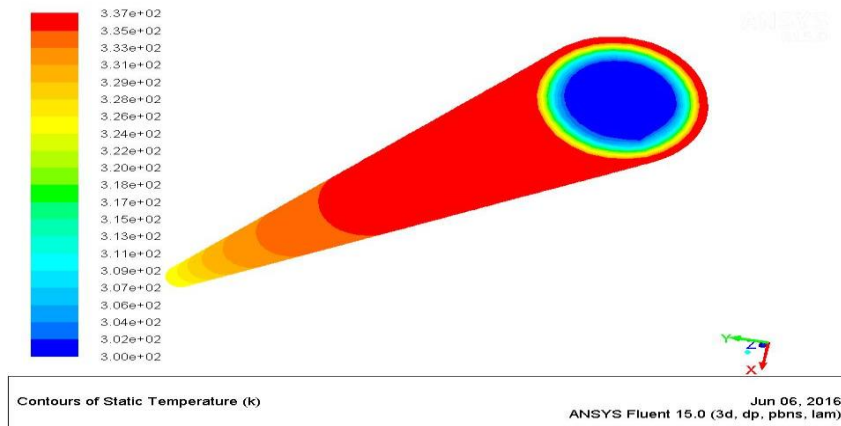


Figure 5.4 Temperature contour when EG flows at 0.11 m/s

In the case 4, temperature rise of a fluid in a single pass is approximately equal to the 3°C. Surface temperature of the tube is approximately equal to 57°C. Maximum temperature of fluid is obtain at the outlet of tube.

Table 5.2 Modelling result with different flow rate of Ethylene Glycol

Flow rate (m/s)	Inlet Temperature	Outlet temperature	Tube Wall Temperature
0.022 (1 LPM)	300 K	308.7 K	337.9 K
0.066 (3 LPM)	300 K	304.9 K	334.8 K
0.11 (5 LPM)	300 K	303.02 K	330.4 K
0.15 (7 LPM)	300 K	302.2 K	327.8 K

5.1.5 Case 5: Therminol VP-1 with flow velocity of 0.066 m/s

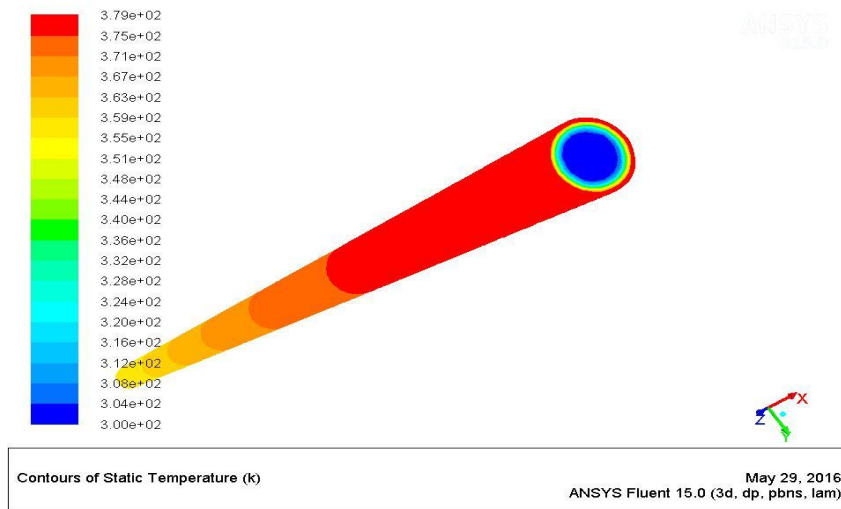


Figure 5.5 Temperature contour when Therminol VP-1 flows at 0.066 m/s

In the case of Therminol oil when it is flows at the rate of 0.066 m/s is high as compare to the another fluids. It is equal to the 6.6 °C in single pass through the tube. Temperature profile of the fluid is shown in the Figure4.9. As the fluid flow velocity increases, then the temperature rise of fluid decreases.

5.1.6 Case 6: Therminol VP-1 with flow velocity of 0.11 m/s

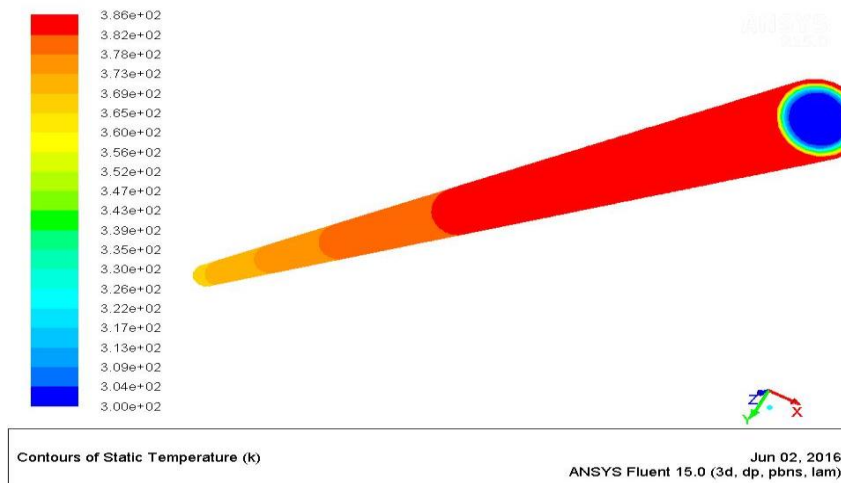


Figure 5.6 Temperature contour when Therminol VP-1 flows at 0.11 m/s

In this case, when the oil flows at the rate of 0.11 m/s the temperature rise in single pass is equal to 4°C. The surface temperature of the tube wall is approximately equal to the 101°C. Trend follows for the temperature gain is similar to the fluid i.e. linearly increases from inlet to outlet section of the tube.

Table 5.3 Modelling result of Therminol VP-1 with different flow rates

Flow rate (m/s)	Inlet Temperature	Outlet temperature	Tube Wall Temperature
0.022 (1 LPM)	300 K	310.79 K	358.5 K
0.066 (3 LPM)	300 K	306.6 K	367.8 K
0.11 (5 LPM)	300 K	304.13 K	376.4 K
0.15 (7 LPM)	300 K	302.79 K	373.8 K

5.1.7 Case 7: Mythol Therm 500 with flow velocity of 0.066 m/s

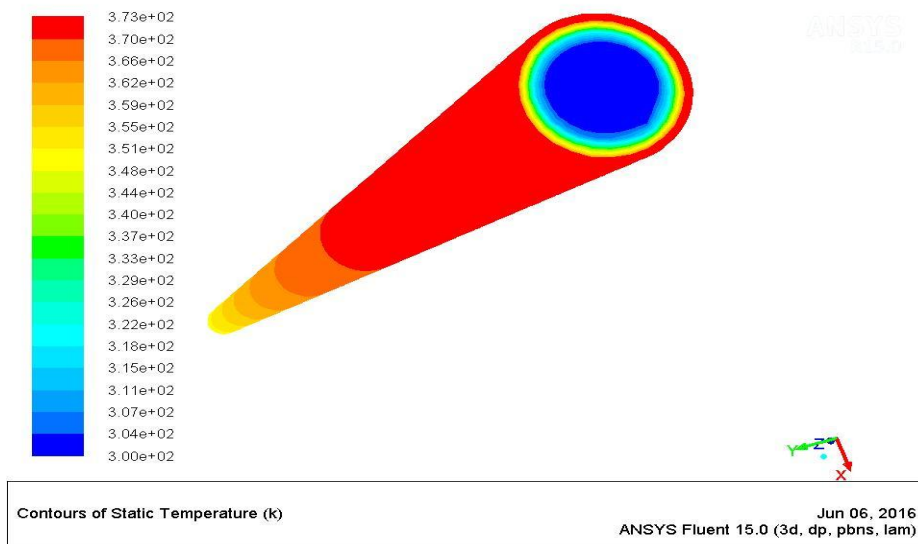


Figure 5.7 Temperature contour when Mythol Therm 500 flows at 0.066 m/s

In this case, temperature contour of heat transfer fluid is shown in Figure 4.11. Temperature of fluid gradually increased from inlet to outlet of pipe similar to another

fluids. Maximum temperature is achieved at the outlet of the heat absorbing tube about 5.8 °C. Surface temperature of the tube wall is equal to the 89°C.

5.1.8 Case 8: Mythol Therm 500 with flow velocity of 0.11 m/s

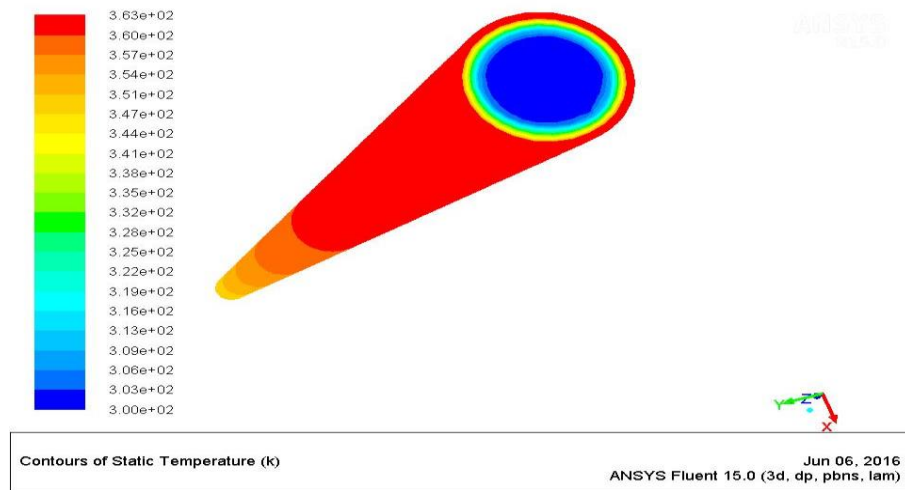


Figure 5.8 Temperature contour when Mythol Therm 500 flows at 0.11 m/s

In the case 8, when the mythol therm oil flows at rate of 0.11 m/s maximum temperature rise in a single pass through the tube is equal to the 3.4 °C and the surface temperature of tube wall is equal to 83°C.

Table 5.4 Modelling result with different flow rates of Mythol Therm 500 oil

Flow rate (m/s)	Inlet Temperature	Outlet temperature	Tube Wall Temperature
0.022 (1 LPM)	300 K	315.7 K	388.1 K
0.066 (3 LPM)	300 K	305.8 K	362.2 K
0.11 (5 LPM)	300 K	303.4 K	356.1 K
0.15 (7 LPM)	300 K	302.3 K	352.3 K

5.2 Experiment Procedure

Step 1: Clean the dust from the reflective surface and absorber tube by using soft cotton cloth and set all measuring instruments accordingly.

Step 2: Set the position of reflecting surface according to the calculated position (solar azimuth) of the sun and turn on the power of pump and tracking mechanism.

Step 3: Set the uniform flow rate of fluid and the system is running on the same flow rate for whole day.

Step 4: The system is running from 10:00 AM to 3:00 PM and readings are taken after every half 'n hour.

Step 5: After 3:00 PM, tracking mechanism and pump is switched off and the whole set up is covered.

Step 6: Heat transfer fluid is changed after reading of two different mass flow rate.

Experimental procedure mentioned in above written steps are repeated for the four different heat transfer fluid.

5.3 Experiment Results

5.3.1 Variation of Output Temperature with Time

Temperature of the fluid increases from its normal value to high value but the trend for variation of the temperature is not same for the different fluid.

5.3.1.1 Case 1: Temperature variation with fluid velocity of 0.066 m/s.

The output temperature of the heat absorbing tube is shown in Figure 5.1, with respect to time interval at velocity of 0.066 m/s of different fluids.

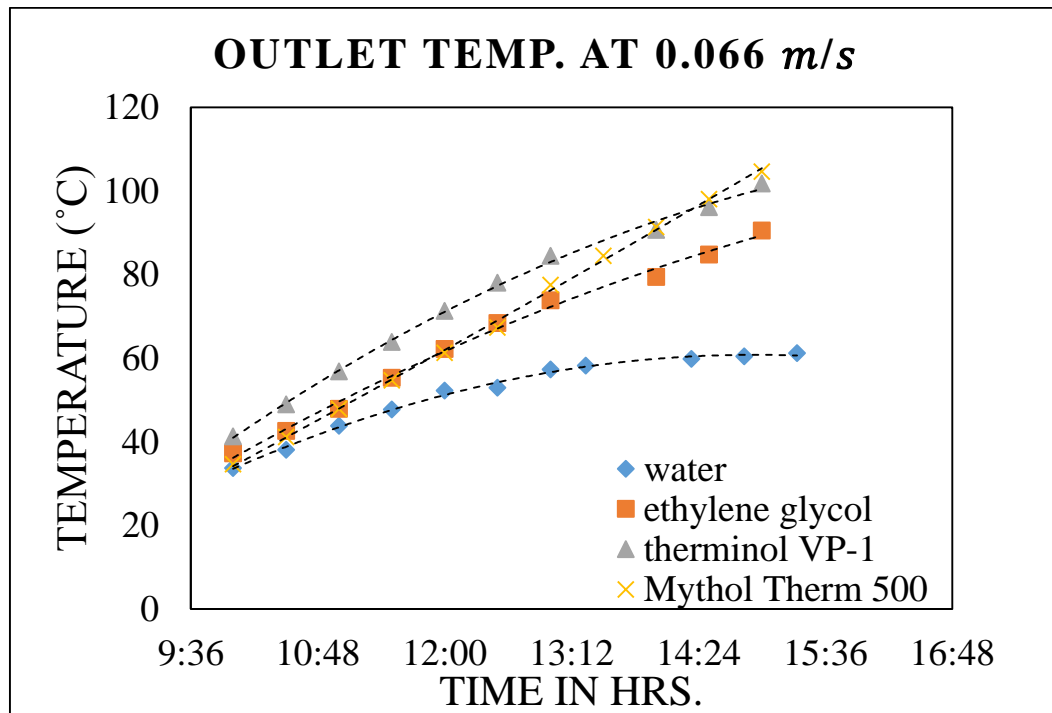


Figure 5.9 Output Temperature of different fluid at velocity 0.066 m/s

Figure 5.1 shows that the resulting output temperature of the heat absorbing fluid at the end of the absorber tube. From the results observed that the maximum temperature rise after the six hours running of the setup is in the Mythol Therm 500 oil is equal to 104.6 °C and the minimum temperature rise in the case of water is approximately equal to the 61.2 °C. Temperature rise in the Therminol Vp-1 oil is equal to the 101.8 °C.

5.3.1.2 Case 2: Temperature variation with the velocity of 0.11 m/s

The output temperature of the heat absorbing tube is shown in Figure 5.2, with respect to time interval at velocity of 0.11 m/s of different fluids.

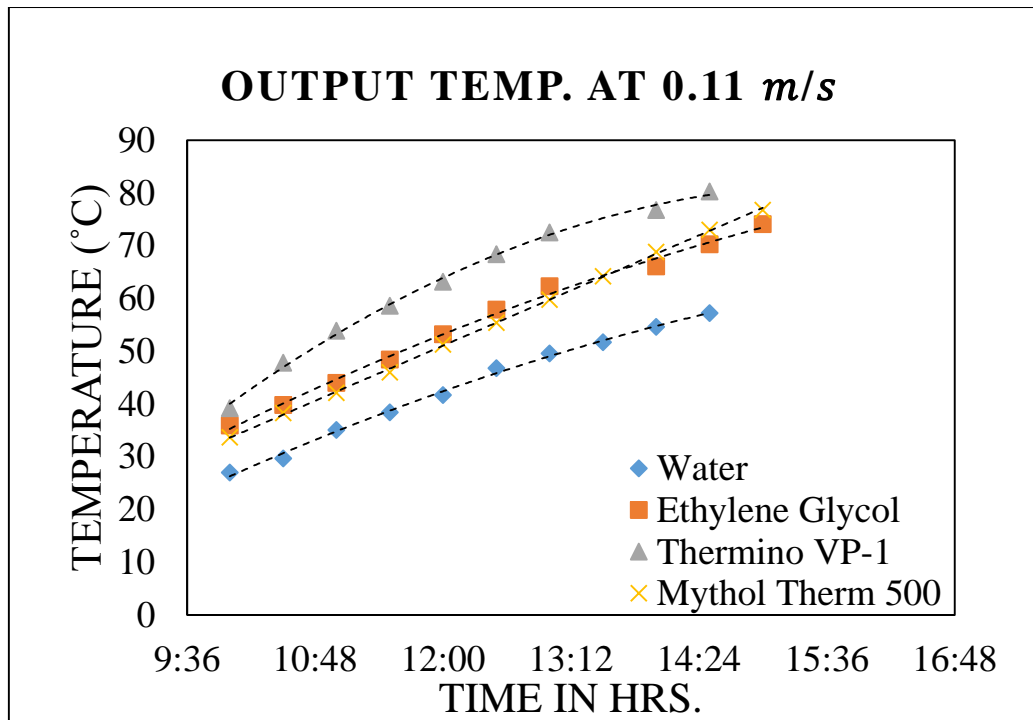


Figure 5.10 Output Temperature of different fluid at velocity 0.11 m/s

Figure 5.2 shows the temperature at the outlet of a heat absorbing tube when the fluid flows at the velocity of 0.11 m/s. Maximum temperature rise is in Therminol Vp-1, it is approximately equal to the 80.3 °C at the outlet and the minimum temperature is rise in the case of water is equal to 57.2 °C after the six hour running of the experiment. Temperature rise in the Mythol Therm 500 oil is 76.8 °C.

From these results observed that, when the fluid velocity is increases then the rise in a temperature is decreases i.e. Temperature rise in a case of 0.066 m/s velocity is more as compare to the temperature rise in the case of 0.11 m/s velocity.

5.3.2 Variation of Efficiency with Time

5.3.2.1 Case 1: Efficiency variation with the velocity 0.066 m/s

Variation of the Efficiency with respect to the time changes in the day at the flow velocity 0.066 m/s of different fluid is as shown in Figure 5.3.

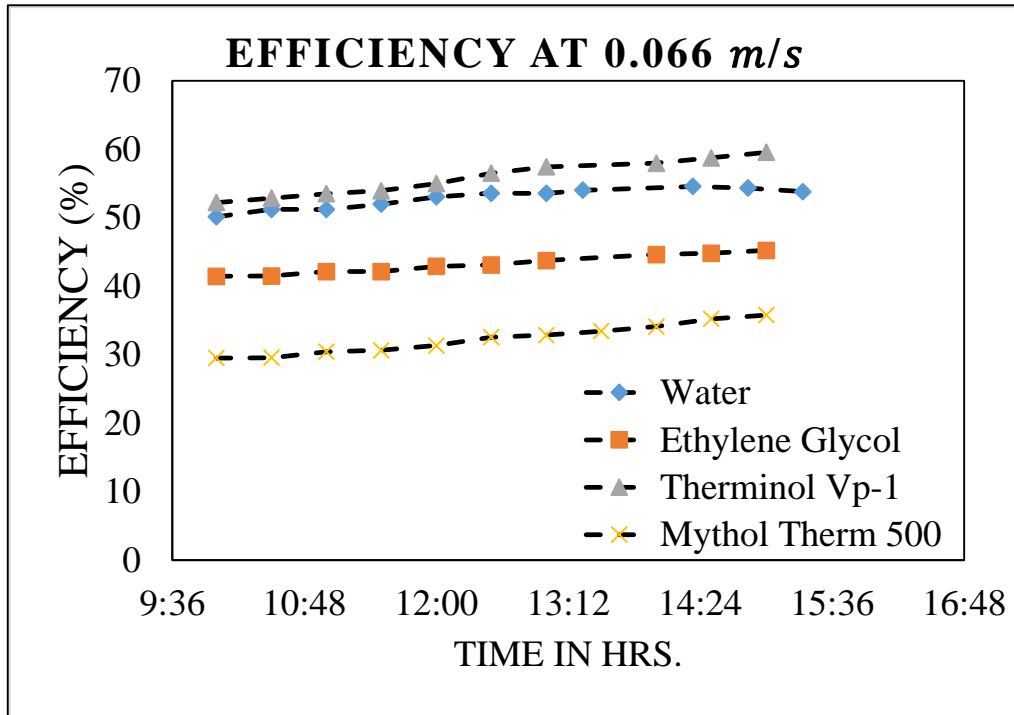


Figure 5.11 Efficiency variation with varying Solar Radiation at day time with velocity 0.066 m/s

Figure 5.3. Indicates the thermal efficiency of a parabolic trough collector by changing the heat transfer fluid with respect to change in the time of day at flow velocity 0.066 m/s. Efficiency of the system is depend upon the so many factors like solar radiation intensity, fluid flow rate, air velocity, thermo-physical properties of fluid etc. With the water PTC has a good thermal efficiency but the temperature rise is less on the same day and Mythol Therm has the efficiency is lower as compare to other fluid but temperature rise is more on same day. The reason for lower efficiency is convective loss is more or high air velocity. By using Therminol VP-1 oil good thermal efficiency is obtained because of its good heat carrying capacity.

5.3.2.2 Case 2: Efficiency variation with velocity of 0.11 m/s.

Variation of the Efficiency with respect to the time changes in the day at the flow velocity 0.11 m/s of different fluid is as shown in Figure 5.4.

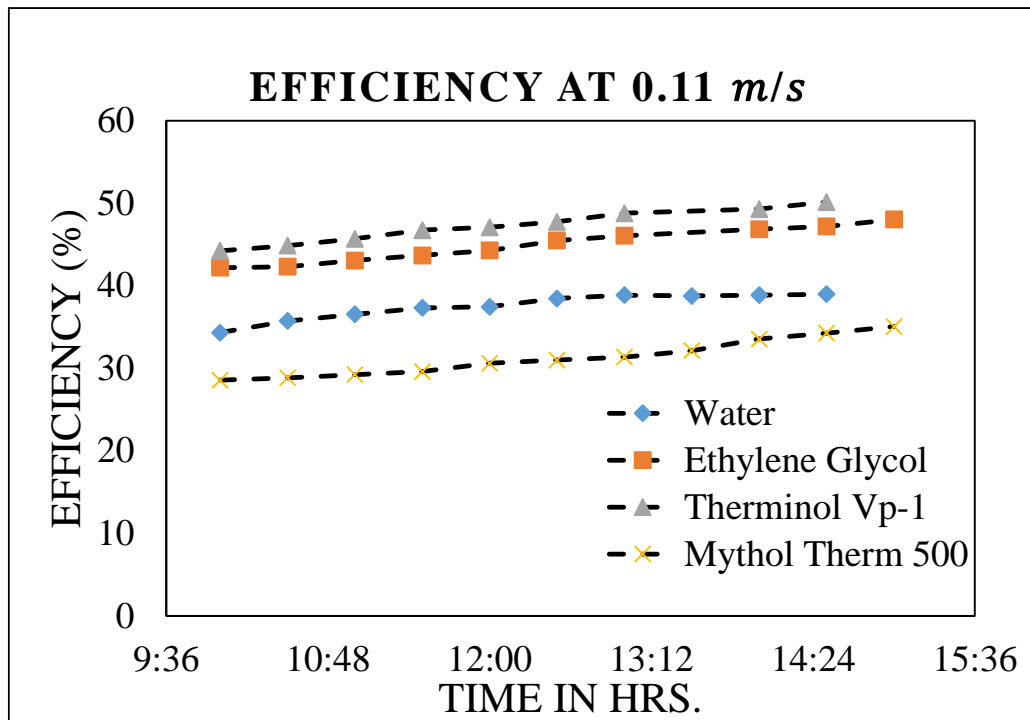


Figure 5.12 Efficiency variation with varying Solar Radiation at day time with velocity 0.11 m/s

Table 5.5 Average efficiency of PTC during Morning, Noon and Full Time

Flow Velocity	0.066 m/s			0.11 m/s		
	Morning Time	Noon Time	Average	Morning Time	Noon Time	Average
Water	49.9 %	51.03 %	52.7 %	36.01 %	37.66 %	46.7 %
Ethylene Glycol	40.34 %	49.62 %	43.9 %	43.83 %	48 %	45.2 %
Therminol VP-1	55.58 %	53.98 %	56.1 %	51.84 %	50.31 %	53.4 %
Mythol Therm 500	33.07 %	33.98 %	33.0 %	33.19 %	30.57 %	32.2 %

As per, Increases the fluid velocity the thermal efficiency of PTC is decreased. In the case of water the thermal efficiency of PTC is decreased more as compare to other fluids by 6 %, In case of ethylene glycol the Efficiency decreased by in range 2 %, In case of Mythol Therm oil and Therminol VP-1 efficiency decreased within range of 3 %.

Averages of the thermal efficiency of the PTC at the day times with fluids are given in the table 5.5.

5.4 Validation with CFD Modeling Results

For the validation of CFD model result, experiment setup is run at the two flow rate 0.066 m/s and 0.11 m/s with four different fluid (water, ethylene glycol, mythol therm 500 oil and Therminol vp-1 oil).

From the experiment results observe that it has a good agreement with CFD model result. These results mostly closer to Model resulting. This indicates that the boundary condition applies in the CFD model and assumptions made to develop this model is closely to the real case.

Energy gain by the heat absorbing fluid is calculated for both of the results comes out by the CFD modeling and experimentation. Graphically representations of the calculation are shown in Figure 5.13. Mythol Therm 500 has a low energy gain with the both fluid velocity (0.066 m/s and 0.11 m/s) as compare to the another HTFs. Hence, its thermal efficiency is low i.e. around 30% to 35 %. Thermal efficiency of a Therminol VP-1 is more among all HTFs used in the experiment and model. It is varies from 50% to 60 % for both fluid velocity and for experiment or CFD model.

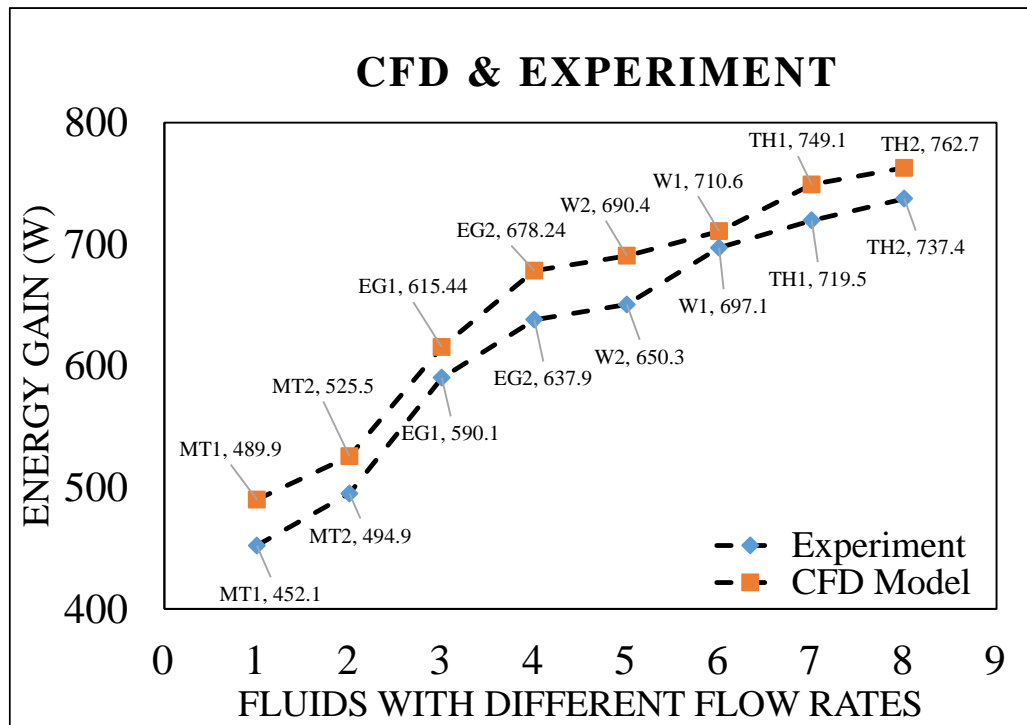


Figure 5.13 Comparison between CFD model and Experimental Energy gain

Table 5.6 Comparison of CFD Model and Experimental Results

Flow Velocity (m/s)	Fluids	CFD Model		Experimental		% Error
		ΔT (K)	Thermal Efficiency (%)	ΔT (K)	Thermal Efficiency (%)	
0.066	Water	3.4	55.9	2.89	52.7	6.7
	Ethylene Glycol	4.9	46.4	4.64	43.9	2.5
	Therminol Vp-1	6.6	59.7	5.83	56.1	6
	Mythol Therm 500	5.8	34.2	5.61	33.0	3.5
0.11	Water	1.9	50.2	1.39	46.7	6.9
	Ethylene Glycol	3.0	46.5	2.92	45.2	2.7
	Therminol Vp-1	4.2	56.6	3.59	53.4	5.6
	Mythol Therm 500	3.4	32.9	3.32	32.2	2.1

Thermal Efficiency of PTC is calculated for the CFD model and Experiment and the relative error between these two. A negligible error is come i.e. reliable. Values of the

percentage error is given in the Table. 5.6. Maximum and minimum thermal efficiency is obtain in Therminol VP-1 and Mythol Therm 500 HTF cases. Water and Ethylene Glycol has intermediate efficiency and the maximum error among all the results are obtain in the case of water as a HTF.

5.5 Summary

The experiments are conducted at two different flow rate for four different type of fluids. The solar radiation intensity, temperature of the HTF at inlet and outlet and fluid velocity are recorded for every set of experiment. The experimental results are used to validate the numerical simulation result. The temperature difference, heat gain and efficiency figures are evaluated and compared. Model simulation results are found to be in close match with the experimental values. The radiation intensity measured during the experiments at 1 PM is found to be deviating from the value used by the radiation model in the CFD simulation, which measures it as per the day and location. Local weather conditions are attributed for the deviation. Also, the wind effect is not modeled into the present study. Though, with evacuated tube cover, the wind losses are not significant in PTC but some differences in model simulation and experimental result is attributed majorly to the wind losses and the deviation in radiation data.

Chapter 6

Conclusions

6.1 Conclusion

The present work has consolidated the modeling study towards design of an absorber tube for a parabolic trough collector with validation of the model with own experiments.

The literature review in present work suggests that a significant amount of experimental work has been performed in the field of solar energy using PTC with variety of heat transfer fluid. The literature related to modeling work is limited towards focus on development of a design specific model.

Present work has identified some research gaps related to modeling towards design of PTC. Present work focuses on the design of absorber tube which functions as heat transfer tube with concentrated solar heat falling on the outer surface and heat being removed through heat transfer fluid (HTF). The design aspect of thermo-physical properties of the HTF, the flow rate and the location of the system installation are majorly focused in the present work. The modeling work need some data to verify the model and author found the lack of all the availability of necessary data in the literature. So, the present thesis also focuses on the experimental work using PTC installed in Energy Lab in Thapar University. The working parameters and the initial and boundary conditions are derived from the own experiments to validate the CFD model developed.

Parabolic trough collector with the reflecting surface of stainless steel material and the material of heat absorbing tube is copper are used in the experiment. Tracking of the collector with respect to the sun position is done by the stepper motor. Which are controlled by the controller. Four types of the heat transfer fluid (Water, Ethylene glycol, Therminol vp-1, Mythol therm 500) are used for testing.

CFD model has been developed for the heat exchanger tube (absorber tube in PTC) using ANSYS computational fluid dynamics software. Geometric modeling has been

done with the dimensions of the absorber tube used in the experimental setup. Fluid velocity and fluid thermo-physical properties has been used as input for the model. Surface to surface radiation module is invoked to simulate the solar energy availability at the local coordinates for a given day. CFD model is simulated for different HTF and varying flow rates and results are analysed. The effects of solar radiation intensity, thermal conductivity, density and specific heat of fluid are studied in detail.

The experiments are conducted at two different flow rate for four different type of fluids. The solar radiation intensity, temperature of the HTF at inlet and outlet and fluid velocity are recorded for every set of experiment. The experimental results are used to validate the numerical simulation result. The temperature difference, heat gain and efficiency figures are evaluated and compared. Model simulation results are found to be in close match with the experimental values. The radiation intensity measured during the experiments at 1 PM is found to be deviating from the value used by the radiation model in the CFD simulation, which measures it as per the day and location. Local weather conditions are attributed for the deviation. Also, the wind effect is not modeled into the present study. Though, with evacuated tube cover, the wind losses are not significant in PTC but some differences in model simulation and experimental result is attributed majorly to the wind losses and the deviation in radiation data.

The present study shows that the thermo-physical properties (density, thermal conductivity and specific heat), location (solar radiation intensity) and fluid flow rate are important design parameters, and found to be sufficient to model the heat receiver tube with significant accuracy and hence to design the system. Depending on the heat gain requirement for a given period of a year, the model can be used to evaluate required length and diameter of tube, material of tube and amount of solar concentration required to achieve the temperature or heat gain with a given HTF towards designing a heat receiver tube.

6.2 Future Scope

Present study has focused mainly on the development of a design philosophy for a heat receiver tube of a PTC. The present work had some constraint in the

experimental work to operate at higher flow rate towards turbulence regime. The receiver tube design was also fixed. Literature suggests that the heat transfer efficiency of the receiver tube increases with the increase in turbulence of the flow and roughness factor inside the tube. Due to lack in flexibility in experiments, the model could not be validated for turbulent flow or high roughness factor of the tube. In future, the studies on the effect of turbulent flow and different tube geometry and roughness factor could be conducted to evaluate the robustness of the model or incorporating changes in model towards universal design of heat receiver tube.

References

- [1] D. John and B. William, Solar engineering and thermal process, fourth edition.
- [2] K. Soteris, “The potential of solar industrial process heat applications” Appl. Energy, vol. 76, pp. 337-361, 2003.
- [3] K. Soteris, “Solar thermal collectors and applications” Progress in Energy and Combustion Science, vol. 30, pp. 231-295, 2004.
- [4] Singh T, “Liquid vapour balance based sun tracking system” Proceedings of the 25th National Renewable Energy Convention of the Solar Society of India, Warangal, India, pp. 401–6, 2001.
- [5] Kearney DW, Price HW, “Solar thermal plants-LUZ concept (current status of the SEGS plants)” Proceedings of the Second Renewable Energy Congress, vol. 2, pp.582-588, 1992.
- [6] Grasse W, Solar PACES annual report, DLR Germany, 1995.
- [7] Verma SK, Tiwari AK, “Progress of Nano fluid application in solar collectors: A review” Energy Conversion and Management, vol. 100, pp. 324-346, 2015.
- [8] Lee JH, Hwang KS, Jang SP, Lee BH, Kim JH, “Effective viscosities and thermal conductivities of aqueous Nano fluids containing low volume concentrations of Al₂O₃ nanoparticles” International Journal of Heat and Mass Transfer, vol. 51, pp. 2651-2656, 2008.
- [9] Choi C, Yoo JM, Oh JM, “Preparation and heat transfer properties of Nano particle in Transformer oil dispersions as advanced energy efficient coolants” Current Applied Physics, Vol. 8, pp. 710-712, 2008.
- [10] Dunn R.I, Hearps PJ, Wright MN, “Molten-Salt Power Towers: Newly Commercial Concentrating Solar Storage” 4 Proceedings of the IEEE, vol. 100, 2012.
- [11] Vignarooban K, Xu X, Arvay A, Hsu K, kannan AM, “Heat transfer fluid for concentrating Solar power systems- A review” Applied Energy, vol. 146, pp. 383-396, 2015.

- [12] Different Radiation model in ANSYS FLUENT, "[FLUENT 6.3 User's Guide - 13.3.1](#)".
- [13] Tian Y, Zhao C.Y, "A review of solar collectors and thermal energy storage in solar thermal applications" Applied Energy, vol. 104, pp. 538-553, 2013.
- [14] Modi A, Haglind F, "Performance analysis of a Kalina cycle for a central receiver solar thermal power plant with direct steam generation" Applied Thermal Engineering, vol. 65, pp. 201-208, 2014.
- [15] Beretta D, Loveless F. C, Nudenberg W, "Use of synthetic hydrocarbon oils as heat transfer fluids" US Patent 4239638, 1980.
- [16] Goods S, Bradshaw R, "Corrosion of stainless steels and carbon steel by molten mixtures of commercial nitrate salts" Journal of Material Engineering and Performance, vol. 13, pp. 78-87, 2004.
- [17] Tijani A S, Roslan Ashraf M. S. B, "Simulation analysis of thermal losses of parabolic trough solar collector in Malaysia using computational fluid dynamics" Procedia Technology, vol. 15, pp. 841-848, 2014.
- [18] He Y, Men Y, Zhao Y, Lu H, Ding Y, "Numerical investigation into the convective heat transfer of TiO₂nanofluid flowing through a straight tube under the laminar flow condition" Applied Thermal Engineering, vol. 29, pp. 1965-1972, 2009.
- [19] Rios-Iribe E. Y, Cervantes-Gaxiola E. Y, Rubio-Castro E, Ponce-Ortega J. M, "Heat transfer analysis of a non-Newtonian fluid flowing through a circular tube with twisted tape inserts" Applied Thermal Engineering, vol. 84, pp. 225-236, 2015.
- [20] Moraveji M. K, Darabi M, Hossein Haddad S. M, Davarnejad R, "Modeling of convective heat transfer of a Nano fluid in the developing region of tube flow with computational fluid dynamics" International Communications in Heat and Mass Transfer, vol. 38, pp.1291-1295, 2011.
- [21] Mwesigye A, Bello-Ochende T, Meyer J. P, "Minimum entropy generation due to heat transfer and fluid friction in a parabolic trough receiver with non-uniform heat flux at different rim angles and concentration ratios" Energy, pp.

1-12, 2014.

- [22] Fard M. H, Esfahany M. N, Talaie M. R, “Numerical study of convective heat transfer of nanofluids in a circular tube two-phase model versus single-phase model” *International Communications in Heat and Mass Transfer*, vol. 37, pp. 91-97, 2010.
- [23] Yaghoubi M, Akbarimoosavi S. M, “3D Thermal- structure analysis of an absorber tube of a parabolic trough collector and the effect of tube deflection on optical efficiency” *Energy Procedia*, vol. 49, pp. 2433-2443, 2014.
- [24] Natarajan M, Sekhar Y. R, Srinivas T, Gupta P, “ Numerical simulation of heat transfer characteristics in the absorber tube of parabolic trough collector with internal flow obstruction” *ARNP Journal of Engineering and Applied Sciences*, vol. 9, pp. 674–681, 2014.
- [25] Anton J. M, Biencinto M, Zarza E, Diez L. E, “Theoretical basis and experimental facility for parabolic trough collectors at high temperature using gas as heat transfer fluid” *Applied Energy*, vol. 135, pp. 373–381, 2014.
- [26] Wu Y. T, Liu S.W, Xiong Y. X, Ding Y. L, “Experimental study on the heat transfer characteristics of a low melting point salt in a parabolic trough solar collector system” *Applied Thermal Engineering*, vol. 89, pp. 748-754, 2015.
- [27] Zhang H, Liang H, You S, “Comparison of different heat transfer models for parabolic trough solar collectors” *Applied Energy*, vol. 148, pp. 105-114, 2015.
- [28] Jiang Y, Zou B, Dong J, Yao Y, “An experimental investigation on a small-sized parabolic trough solar collector for water heating in cold areas” *Applied Energy*, vol. 163, pp. 396-407, 2016.
- [29] Behar O, Khellaf A, Mohammedi K, “A novel parabolic trough solar collector model Validation with experimental data and comparison to Engineering Equation Solver (EES)” *Energy Conversion and Management*, vol. 106, pp. 268-281, 2015.
- [30] Shafii M. B, Mosleh H. J, Sima A. H, “A new desalination system using a combination of heat pipe, evacuated tube and parabolic trough collector”

Energy Conversion and Management, vol. 99, pp. 141-150, 2015.

- [31] Larcher M, Rommel M, Bohren A, Frank E, Minder S, “Characterization of a parabolic trough collector for process heat applications” Energy Procedia, vol. 57, pp. 2804-2811, 2014.
- [32] Alguacil M, Prieto C, Rodriguez A, Lohr J, “Direct steam generation in parabolic trough collector” Energy Procedia, vol.49, pp. 21-29, 2014.
- [33] Cheng Z. D, He Y. L, Wang K, Du B.C,Cui F.Q, “A detailed parameter study on the comprehensive characteristics and performance of a parabolic trough solar collector system” Applied Thermal Engineering., vol. 63, pp. 278–289, 2014.

Appendix A

Table A.1 Water with flow rate 0.066 m/s

Day Time (Hrs.)	Atmospheric Temperature (K)	Inlet Temperature (K)	Outlet Temperature (K)	Solar Intensity (W/m ²)	Efficiency (%)
10:00	296.95	304.15	306.85	528.8	54.17
10:30	298.75	308.35	311.25	582.8	53.07
11:00	300.45	313.85	316.95	624.8	52.92
11:30	302.35	318.55	320.85	645.7	37.39
12:00	303.55	321.95	325.35	676.4	51.94
12:30	303.35	323.55	326.05	688.8	37.78
13:00	304.35	327.05	330.45	676.9	52.28
13:20	304.55	328.35	331.35	631.6	49.44
14:20	304.85	329.75	332.95	610.6	54.55
14:50	305.55	330.75	333.55	559.4	52.54
15:20	305.85	331.85	334.35	501.4	53.62

Table A.2 Ethylene Glycol with flow rate 0.066 m/s

Day Time (Hrs.)	Atmospheric Temperature (K)	Inlet Temperature (K)	Outlet Temperature (K)	Solar Intensity (W/m ²)	Efficiency (%)
10:00	315.35	306.15	310.35	668.25	41.47
10:30	315.05	311.25	315.75	715.5	41.50
11:00	313.25	316.55	321.05	813.75	36.49
11:30	314.35	323.95	328.45	821.25	36.48
12:00	312.75	330.55	335.35	848.25	45.79
12:30	313.25	336.55	341.55	761.25	48.99
13:00	315.45	342.35	346.95	828.75	41.09
14:00	314.25	347.75	352.55	696	53.59
14:30	313.85	353.35	357.95	684	52.88
15:00	313.35	358.75	363.65	634.5	61.59

Table A.3 Therminol VP-1 with flow rate 0.066 m/s

Day Time (Hrs.)	Atmospheric Temperature (K)	Inlet Temperature (K)	Outlet Temperature (K)	Solar Intensity (W/m ²)	Efficiency (%)
10:00	313.95	308.95	314.45	635.6	52.23
10:30	316.75	316.25	322.05	697.2	55.76
11:00	315.15	323.65	329.95	753.2	58.00
11:30	314.55	330.85	337.05	730.4	56.90
12:00	312.65	338.15	344.45	731.5	55.01
12:30	312.35	345.25	351.15	697.7	56.54
13:00	314.35	351.65	357.65	700.4	52.15
14:00	315.25	358.05	363.85	676.9	52.97
14:30	314.95	363.85	369.25	599.2	53.51
15:00	315.45	369.85	374.95	575.9	54.75

Table A.4 Mythol Therm 500 with flow rate 0.066 m/s

Day Time (Hrs.)	Atmospheric Temperature (K)	Inlet Temperature (K)	Outlet Temperature (K)	Solar Intensity (W/m ²)	Efficiency (%)
10:00	302.95	302.15	307.75	669	37.10
10:30	304.25	308.85	314.25	730.5	37.38
11:00	304.85	315.45	321.05	794.25	31.52
11:30	306.25	321.95	327.85	825.75	29.59
12:00	306.85	328.85	334.45	847.5	29.78
12:30	309.05	335.25	340.45	830.25	32.58
13:00	308.95	345.35	350.65	849.75	30.85
13:30	308.45	351.95	357.65	808.5	31.52
14:00	308.15	358.75	364.55	768	30.75
14:30	308.55	365.25	371.15	686.25	36.54
15:00	308.85	371.95	377.75	617.25	41.65

Appendix B

Table B.1 Water with flow rate 0.11 m/s

Day Time (Hrs.)	Atmospheric Temperature (K)	Inlet Temperature (K)	Outlet Temperature (K)	Solar Intensity (W/m ²)	Efficiency (%)
10:00	298.15	299.05	300.15	562.5	34.32
10:30	299.55	301.45	302.85	600	40.94
11:00	300.95	306.95	308.25	633.75	36.52
11:30	300.65	310.05	311.55	682.5	38.95
12:00	301.95	313.65	314.85	725.25	29.32
12:30	302.55	318.35	319.95	723.75	38.60
13:00	302.65	321.25	322.75	737.25	36.23
13:30	303.45	323.45	324.85	690	36.31
14:00	304.25	326.25	327.75	684	38.86
14:30	303.85	328.95	330.35	648	38.29

Table B.2 Ethylene Glycol with flow rate 0.11 m/s

Day Time (Hrs.)	Atmospheric Temperature (K)	Inlet Temperature (K)	Outlet Temperature (K)	Solar Intensity (W/m ²)	Efficiency (%)
10:00	311.45	306.45	309.05	712.5	44.60
10:30	310.65	310.25	312.95	765.75	42.29
11:00	312.05	314.45	317.15	806.25	40.16
11:30	312.55	318.65	321.55	800.25	43.67
12:00	311.35	323.15	326.35	784.5	48.45
12:30	312.35	327.75	331.05	787.5	49.77
13:00	313.35	332.35	335.45	825.75	44.59
14:00	313.85	336.35	339.25	781.5	45.14
14:30	313.25	340.35	343.45	713.25	49.88
15:00	313.05	344.55	347.25	636.75	50.61

Table B.3 Therminol VP-1 with flow rate 0.11 m/s

Day Time (Hrs.)	Atmospheric Temperature (K)	Inlet Temperature (K)	Outlet Temperature (K)	Solar Intensity (W/m ²)	Efficiency (%)
10:00	310.85	309.35	312.35	600.75	51.21
10:30	311.25	317.55	320.95	643.5	53.77
11:00	312.65	323.25	327.05	682.5	51.95
11:30	313.05	327.95	331.75	737.25	49.89
12:00	313.95	332.55	336.35	741.75	52.40
12:30	314.05	337.45	341.55	766.5	48.83
13:00	312.35	342.05	345.65	717.75	49.80
14:00	315.05	346.35	349.95	703.5	49.28
14:30	317.15	350.25	353.45	610.5	53.35

Table B.4 Mythol Therm 500 with flow rate 0.11 m/s

Day Time (Hrs.)	Atmospheric Temperature (K)	Inlet Temperature (K)	Outlet Temperature (K)	Solar Intensity (W/m ²)	Efficiency (%)
10:00	302.15	303.65	306.85	694.5	34.10
10:30	303.75	308.05	311.45	756	32.62
11:00	304.95	312.35	315.25	804	28.68
11:30	305.65	316.15	319.15	822.75	28.59
12:00	306.95	320.95	324.45	617.06	41.98
12:30	307.45	325.25	328.55	898.5	28.39
13:00	308.45	329.35	332.95	858	29.82
13:30	308.55	333.85	337.35	843.75	28.88
14:00	309.15	338.45	341.95	833.25	29.54
14:30	309.65	342.75	346.15	746.25	31.72
15:00	309.95	346.75	349.95	675.75	35.05